

Synthesis of a Bimetallic Dodecaborate $\text{LiNaB}_{12}\text{H}_{12}$ with Outstanding Superionic Conductivity

Liqing He,[†] Hai-Wen Li,^{*,‡,§} Hironori Nakajima,^{†,§} Nikolay Tumanov,[⊥] Yaroslav Filinchuk,^{*,⊥} Son-Jong Hwang,[#] Manish Sharma,^{||} Hans Hagemann,^{||} and Etsuo Akiba^{†,‡,§}

[†]Department of Mechanical Engineering, [‡]International Research Center for Hydrogen Energy, and [§]WPI International Institute for Carbon-Neutral Energy Research (WPI-I2CNER), Kyushu University, Fukuoka 819-0395, Japan

[⊥]Institute of Condensed Matter and Nanosciences, Université catholique de Louvain, Louvain-la-Neuve 1348, Belgium

[#]Division of Chemistry and Chemical Engineering, California Institute of Technology, Pasadena, California 91125, United States

^{||}Département de Chimie Physique, Université de Genève, CH1211 Geneva 4, Switzerland

S Supporting Information

Metal dodecaborates $\text{M}_{2/n}\text{B}_{12}\text{H}_{12}$ (n denotes the valence of the metal M), containing icosahedral polyatomic anion $[\text{B}_{12}\text{H}_{12}]^{2-}$, have been attracting increasing interest as potential energy materials, especially in the context of hydrogen storage^{1,2} and superionic conductivity.³ $\text{M}_{2/n}\text{B}_{12}\text{H}_{12}$ are commonly formed as dehydrogenation intermediates from metal borohydrides $\text{M}(\text{BH}_4)_n$, like LiBH_4 and $\text{Mg}(\text{BH}_4)_2$,^{4–8} which are well-known as potential high-density hydrogen storage materials.^{9–11} The strong B–B bond in the icosahedral $[\text{B}_{12}\text{H}_{12}]^{2-}$, however, is regarded to be the key factor that prevents the rehydrogenation of dodecaborates.¹² In order to elucidate the mechanism as well as to provide effective solutions to this problem, a novel solvent-free synthesis route of anhydrous $\text{M}_{2/n}\text{B}_{12}\text{H}_{12}$ (here M means Li, Na, and K) has been developed.¹³ Thermal stability and transformations of the anhydrous single phase $\text{Li}_2\text{B}_{12}\text{H}_{12}$ suggested the formation of the high temperature polymorph of $\text{Li}_2\text{B}_{12}\text{H}_{12}$ during the dehydrogenation of LiBH_4 , while concurrently emphasized the importance of further investigation on the decomposition mechanism of metal borohydrides and metal dodecaborates.¹⁴ The high stability of icosahedral $[\text{B}_{12}\text{H}_{12}]^{2-}$, on the other hand, favors its potential application as solid electrolyte. Recently, Na^+ conductivity of $\text{Na}_2\text{B}_{12}\text{H}_{12}$ was reported to be 0.1 S/cm above its order–disorder phase transition at ~ 529 K,³ which is comparable to that of a polycrystalline $\beta''\text{-Al}_2\text{O}_3$ (0.24 S/cm at 573 K) solid state Na-electrolyte.¹⁵ Mechanistic understanding on the diffusion behavior of cation and further improvement of ionic conductivity at a lower temperature, however, are important in order to facilitate the practical application of metal dodecaborates as superionic conductors.

Bimetallic compounds composed of two different metal elements often show different crystal structures and interesting chemical and physical properties, which are often distinguished from those of the monometallic counterparts. For example, bimetallic borohydrides have been proven as a way to tune the thermodynamics of metal borohydride decomposition.^{16–18} To our best knowledge, there has been no report of improving the ionic conductivity of $\text{M}_{2/n}\text{B}_{12}\text{H}_{12}$ by introducing another metal to form a bimetallic dodecaborate, and we hypothesized that the coexistence of bimetallic elements could have a synergetic effect on the mobility change of each ion. Here we report for the first time that a bimetallic dodecaborate $\text{LiNaB}_{12}\text{H}_{12}$ could

be a model system in demonstrating the hypothesis, exhibiting lower phase transition temperature (488 K) than its single counterparts of $\text{Li}_2\text{B}_{12}\text{H}_{12}$ (615 K) and $\text{Na}_2\text{B}_{12}\text{H}_{12}$ (529 K),¹⁹ and the ionic conductivity of $\text{LiNaB}_{12}\text{H}_{12}$ reaches a value of 0.79 S/cm at 550 K. The conductivity value is approximately 8 times higher than that of $\text{Na}_2\text{B}_{12}\text{H}_{12}$ ³ and 11 times higher than that of $\text{Li}_2\text{B}_{12}\text{H}_{12}$ at the same temperature.

$\text{LiNaB}_{12}\text{H}_{12}$ was prepared through sintering of LiBH_4 , NaBH_4 , and $\text{B}_{10}\text{H}_{14}$ with a stoichiometric molar ratio of 1:1:1. The successful synthesis was confirmed by X-ray diffraction, Raman spectra, and solid state nuclear magnetic resonance (NMR) measurements (see Supporting Information Figure S1). The phase transition of $\text{LiNaB}_{12}\text{H}_{12}$, examined by differential scanning calorimetry (DSC) (Figure 1), occurs at

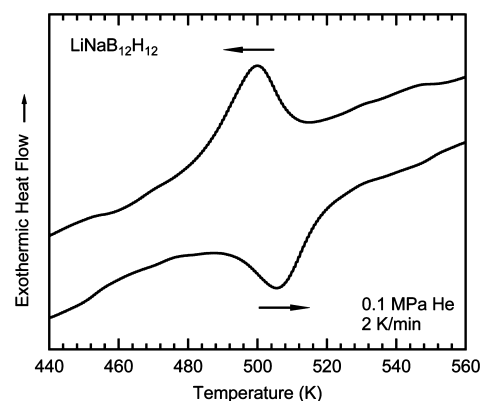


Figure 1. Differential scanning calorimetry curves showing the reversible phase transition in $\text{LiNaB}_{12}\text{H}_{12}$.

the temperature of 488 K, which is substantially lower than those reported for pure $\text{Li}_2\text{B}_{12}\text{H}_{12}$ (615 K) and $\text{Na}_2\text{B}_{12}\text{H}_{12}$ (529 K).¹⁹ The heats for phase transitions of $\text{LiNaB}_{12}\text{H}_{12}$, $\text{Li}_2\text{B}_{12}\text{H}_{12}$, and $\text{Na}_2\text{B}_{12}\text{H}_{12}$ are determined as 9, 22, and 11 kJ/mol, respectively, based on the DSC measurements (not shown), suggesting that $\text{LiNaB}_{12}\text{H}_{12}$ thermodynamically favors the

Received: April 28, 2015

Revised: August 6, 2015

Published: August 7, 2015

phase transition compared to $\text{Li}_2\text{B}_{12}\text{H}_{12}$ and $\text{Na}_2\text{B}_{12}\text{H}_{12}$. It is worth emphasizing that there is no obvious change of the phase transition in $\text{LiNaB}_{12}\text{H}_{12}$ even after 20 cycles of heating and cooling measurements (see Supporting Information Figure S2), whereas a partial decomposition is clearly observed in $\text{Li}_2\text{B}_{12}\text{H}_{12}$ and $\text{Na}_2\text{B}_{12}\text{H}_{12}$.¹⁹

The structural investigations of $\text{LiNaB}_{12}\text{H}_{12}$ by synchrotron X-ray powder diffraction were performed in the range 298–613 K (see Supporting Information Figures S3 and S4 for Rietveld plots of low- and high-temperature phases). The low temperature structure reveals the cubic $P\bar{a}3$ space group symmetry with the cell parameter $a = 9.8009(1)$ Å at 298 K, isostructural to the low- T phase of $\text{Li}_2\text{B}_{12}\text{H}_{12}$.²⁰ The high- T structure shows a cubic F -centered unit cell. The result is different from the behavior of $\text{Li}_2\text{B}_{12}\text{H}_{12}$, for which the high- T phase was described in the literature as disordered structure in the parent primitive cubic cell.²¹ We searched further for a better structural model of the high- T phase and found that the high- T phase is better matched with a space group symmetry $Fm\bar{3}m$ where both metal and $[\text{B}_{12}\text{H}_{12}]^{2-}$ sites are disordered. The Li/Na mixed-metal site is a stronger scatterer than Li only, which helped us to determine that the unit cell of the high- T phase is clearly F -centered antifluorite structure. We suppose that the high- T phase of $\text{LiNaB}_{12}\text{H}_{12}$ is isostructural to the high- T phase of $\text{Li}_2\text{B}_{12}\text{H}_{12}$,²¹ but we and the authors of the past work are using two different models for the description of the same highly disordered structure. Our refinements show a significant positional disorder on the Li/Na site centered at the 8-fold $1/4$ $1/4$ $1/4$ position; the dodecaborane anions are centered at the 4-fold 0 0 0 position. The anions may be positionally ordered, especially in the F -centered cubic subgroups of $Fm\bar{3}m$. Interestingly, the antifluorite structure is known to be favorable for superionic conductivity, demonstrated by Na_2S .²²

The temperature-induced phase transition is reversible, a sequential refinement was done on 313 powder patterns collected, and the cell parameters of the two phases are plotted as a function of T in Figure 2. The unit cell parameters show practically linear T dependences. The phase transition happens at 514 K on heating and at 481 K on cooling, and the cell parameters exhibit nearly the same values (ca. 0.13 Å) of expansion or shrinkage on heating or cooling. Thus, we can state that no hydrogen desorption/absorption occurs at 16.0

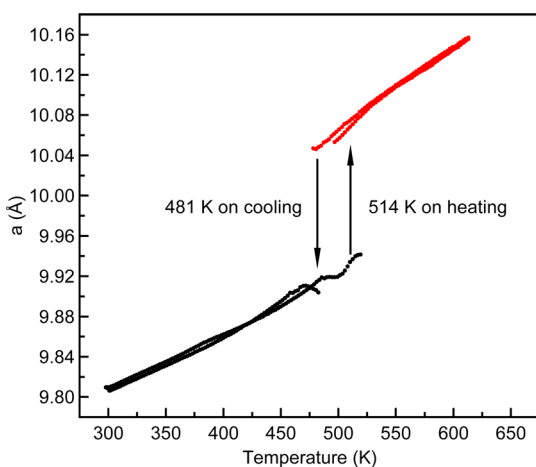


Figure 2. Unit cell dimension of $\text{LiNaB}_{12}\text{H}_{12}$ as a function of temperature, refined from the in situ synchrotron X-ray diffraction profiles measured at 16.0 MPa H_2 with a heating rate of 5 K/min.

MPa H_2 and temperatures up to 773 K. A similar experiment without hydrogen back pressure shows that hydrogen has no significant effect on the phase transition; the phase transition occurs at 514 K on heating and at 481 K on cooling, and no hydrogen desorption/absorption was observed.

The reversible phase transition is also examined by the in situ Raman spectroscopy measurements as shown in Figure 3.

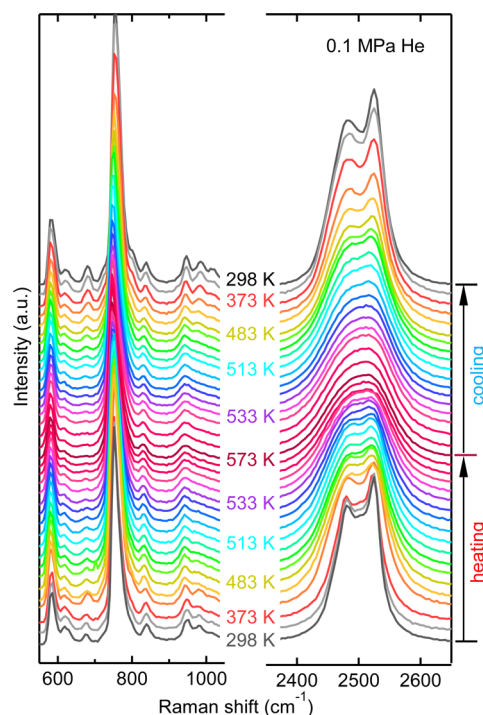


Figure 3. In situ Raman spectra of $\text{LiNaB}_{12}\text{H}_{12}$ upon heating and cooling at 0.1 MPa He.

When the temperature is increased above the phase transition temperature, the B–H bending modes at 618, 680, and 980 cm^{-1} start to disappear at 513 K, the two B–H stretching mode peaks at around 2500 cm^{-1} start to merge, and a single peak is observed at 553 K due to the disordered structure of the high- T phase. When the temperature is decreased below the phase transition temperature (Figure 3), the bending modes at 618, 680, and 980 cm^{-1} reappear, and the stretching band around 2500 cm^{-1} splits into two peaks. DFT calculations on isolated $\text{B}_{12}\text{H}_{12}^{2-}$ and $\text{Li}_2\text{B}_{12}\text{H}_{12}$ (with D_{3d} symmetry, to be as close as possible to the S_6 local symmetry in the $\text{LiNaB}_{12}\text{H}_{12}$ crystal) were performed to further analyze the origin of these bands. It appears in particular that the band at 680 cm^{-1} , which is not observed in the Raman spectrum of the cubic $\text{Cs}_2\text{B}_{12}\text{H}_{12}$,²³ originates from a Raman inactive mode with G_g symmetry for the icosahedral $\text{B}_{12}\text{H}_{12}^{2-}$ anion (see the gif animation in the Supporting Information). The calculated frequencies and experimental Raman frequencies are summarized in the Supporting Information. It is also important to note that the space groups $Fm\bar{3}m$ and $P\bar{a}3$ do not have a direct group–subgroup relation. This fact leads to the hysteresis shown in Figure 2 but is also reflected by the fact that the band at 680 cm^{-1} disappears suddenly at the phase transition with increasing temperature.

Ionic conductivities of $\text{LiNaB}_{12}\text{H}_{12}$ measured by an electrochemical impedance spectroscopy (see Supporting Information, Figure S5) display a significant increase with temperature

(Figure 4): above the phase transition temperature it is 6 orders of magnitude higher than that at room temperature. At 550 K

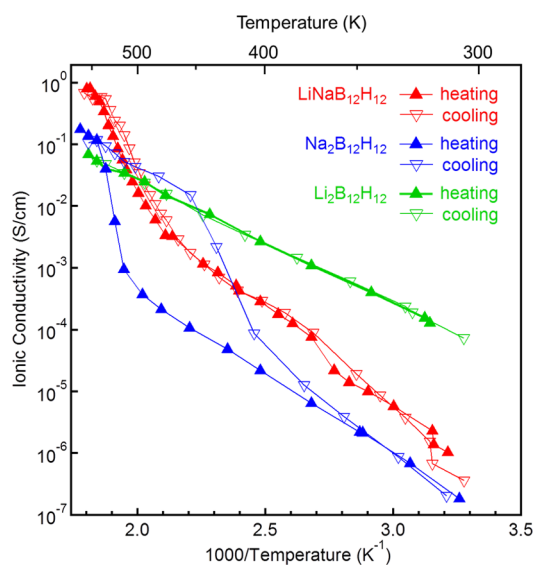


Figure 4. Ionic conductivity measurements for $\text{LiNaB}_{12}\text{H}_{12}$, $\text{Na}_2\text{B}_{12}\text{H}_{12}$, and $\text{Li}_2\text{B}_{12}\text{H}_{12}$ as a function of temperature.

the ionic conductivity reaches 0.79 S/cm, which is approximately 8 and 11 times higher than those for the monometallic systems such as $\text{Na}_2\text{B}_{12}\text{H}_{12}$ ³ and $\text{Li}_2\text{B}_{12}\text{H}_{12}$, respectively. Note further that below the phase transition temperature of 488 K, the ionic conductivity of $\text{LiNaB}_{12}\text{H}_{12}$ is in between those of $\text{Na}_2\text{B}_{12}\text{H}_{12}$ and of $\text{Li}_2\text{B}_{12}\text{H}_{12}$. Li ionic transport number estimated using polarization responses (see Supporting Information Figure S6) decreases from 0.91 to 0.71 with temperature increased from 393 to 433 K, implying that Li^+ contributes much more than Na^+ to the superionic conductivity, but its fraction decreases at elevated temperature. In addition, unlike $\text{Na}_2\text{B}_{12}\text{H}_{12}$ in this work and in the earlier reported studies,³ a much smaller hysteretic behavior is observed for $\text{LiNaB}_{12}\text{H}_{12}$ during the cooling process. The significantly improved ionic conductivity and the minimal hysteresis behavior demonstrated by the $\text{LiNaB}_{12}\text{H}_{12}$, therefore, prove the synergistic effects of the two metals in the bimetallic dodecaborate. This case further shows the feasibility of designing bimetallic dodecaborates to tune geometric structure and to improve the ion mobility. Further investigation on $\text{LiNaB}_{12}\text{H}_{12}$ with different molar ratios of Li/Na, as well as various bimetallic systems with different ionic radius and valence, is of great importance for the clarification of the detailed mechanism and the improvement of ionic conductivity at moderate temperature for the application of metal dodecaborates as solid electrolyte for batteries.

In conclusion, for the first time we have successfully synthesized the bimetallic dodecaborate, $\text{LiNaB}_{12}\text{H}_{12}$, through sintering LiBH_4 , NaBH_4 , and $\text{B}_{10}\text{H}_{14}$, showing the feasibility of this process for syntheses of bimetallic dodecaborate series containing no crystal water. The bimetallic series may comprise alkali-earth and transition metals, which are in great need for developing advanced solid state electrolytes and high density hydrogen storage materials. The bimetallic dodecaborate $\text{LiNaB}_{12}\text{H}_{12}$ exhibits lower phase transition temperature, smaller hysteresis, and significantly higher ionic conductivity than its monometallic counterparts, i.e., $\text{Li}_2\text{B}_{12}\text{H}_{12}$ and

$\text{Na}_2\text{B}_{12}\text{H}_{12}$. The revealed Li/Na compositional disorder and the related positional disorder on the metal site are likely responsible for the improved superionic conductivity of $\text{LiNaB}_{12}\text{H}_{12}$. These interesting results demonstrate our strategy of bimetallic dodecaborates to be effective in improving the ionic conductivity.

■ ASSOCIATED CONTENT

Supporting Information

The Supporting Information is available free of charge on the ACS Publications website at DOI: 10.1021/acs.chemmater.5b01568.

Experimental procedures including material synthesis and characterization methods, XRD, Raman and NMR for the material synthesis, 20 cycles of heating and cooling DSC curves, high-resolution X-ray powder diffraction, and electrochemical impedance measurement. Calculated and observed Raman frequencies and correlation table for the Ih group. (PDF)
DFT calculated structure of $\text{Li}_2\text{B}_{12}\text{H}_{12}$ (GIF)

■ AUTHOR INFORMATION

Corresponding Authors

*(H.L.) E-mail: li.haiwen.305@m.kyushu-u.ac.jp.

*(Y.F.) E-mail: yaroslav.flinchuk@uclouvain.be.

Author Contributions

The manuscript was written through contributions of all authors. All authors have given approval to the final version of the manuscript.

Funding

This work was partly supported by Grants-in-Aid for Scientific Research No. 25709067, JSPS Invitation Fellowship for Research in Japan (Short-Term), the International Institute for Carbon Neutral Energy Research (WPI-I2CNER), sponsored by the Japanese Ministry of Education, Culture, Sports, Science and Technology of Japan, Fonds Spéciaux de Recherche and FNRS as well as SNBL (ESRF) for the beamtime, and the Swiss National Science Foundation. The NMR facility at Caltech was supported by the National Science Foundation (NSF) under Grant Number 9724240 and partially supported by the MRSEC Program of the NSF under Award Number DMR-520565.

Notes

The authors declare no competing financial interest.

■ REFERENCES

- Li, H.-W.; Yan, Y.; Orimo, S.-i.; Züttel, A.; Jensen, C. M. Recent progress in metal borohydrides for hydrogen storage. *Energies* **2011**, *4*, 185–214.
- Jena, P. Superhalogens—a bridge between complex metal hydrides and Li-ion batteries. *J. Phys. Chem. Lett.* **2015**, *6*, 1119–1125.
- Udovic, T. J.; Matsuo, M.; Unemoto, A.; Verdal, N.; Stavila, V.; Skripov, A. V.; Rush, J. J.; Takamura, H.; Orimo, S.-i. Sodium superionic conduction in $\text{Na}_2\text{B}_{12}\text{H}_{12}$. *Chem. Commun.* **2014**, *50*, 3750–3752.
- Orimo, S.-i.; Nakamori, Y.; Ohba, N.; Miwa, K.; Aoki, M.; Towata, S.-i.; Züttel, A. Experimental studies on intermediate compound of LiBH_4 . *Appl. Phys. Lett.* **2006**, *89*, 021920.
- Li, H.-W.; Kikuchi, K.; Nakamori, Y.; Ohba, N.; Miwa, K.; Towata, S.; Orimo, S. Dehydrogenating and rehydrogenating processes of well-crystallized $\text{Mg}(\text{BH}_4)_2$ accompanying with formation of intermediate compounds. *Acta Mater.* **2008**, *56*, 1342–1347.

(6) Hwang, S.-J.; Bowman, R. C.; Reiter, J. W.; Rijssenbeek, J.; Soloveichik, G. L.; Zhao, J.-C.; Kabbour, H.; Ahn, C. C. NMR confirmation for formation of $[\text{B}_{12}\text{H}_{12}]^{2-}$ complexes during hydrogen desorption from metal borohydrides. *J. Phys. Chem. C* **2008**, *112*, 3164–3169.

(7) Friedrichs, O.; Remhof, A.; Hwang, S.-J.; Züttel, A. Role of $\text{Li}_2\text{B}_{12}\text{H}_{12}$ for the formation and decomposition of LiBH_4 . *Chem. Mater.* **2010**, *22*, 3265–3268.

(8) Ozolins, V.; Majzoub, E.; Wolverton, C. First-principles prediction of thermodynamically reversible hydrogen storage reactions in the Li-Mg-Ca-B-H system. *J. Am. Chem. Soc.* **2009**, *131*, 230–237.

(9) Züttel, A.; Wenger, P.; Rentsch, S.; Sudan, P.; Mauron, P.; Emmenegger, C. LiBH_4 a new hydrogen storage material. *J. Power Sources* **2003**, *118*, 1–7.

(10) Filinchuk, Y.; Richter, B.; Jensen, T. R.; Dmitriev, V.; Chernyshov, D.; Hagemann, H. Porous and dense magnesium borohydride frameworks: synthesis, stability, and reversible absorption of guest species. *Angew. Chem., Int. Ed.* **2011**, *50*, 11162–11166.

(11) Schouwink, P.; Ley, M. B.; Tissot, A.; Hagemann, H.; Jensen, T. R.; Smrčok, L.; Černý, R. Structure and properties of complex hydride perovskite materials. *Nat. Commun.* **2014**, *5*, 5706.

(12) Li, H.-W.; Akiba, E.; Orimo, S.-i. Comparative study on the reversibility of pure metal borohydrides. *J. Alloys Compd.* **2013**, *580*, S292–S295.

(13) He, L.; Li, H.-W.; Hwang, S.-J.; Akiba, E. Facile Solvent-Free Synthesis of anhydrous alkali metal dodecaborate $\text{M}_2\text{B}_{12}\text{H}_{12}$ (M= Li, Na, K). *J. Phys. Chem. C* **2014**, *118*, 6084–6089.

(14) Pitt, M. P.; Paskevicius, M.; Brown, D. H.; Sheppard, D. A.; Buckley, C. E. Thermal stability of $\text{Li}_2\text{B}_{12}\text{H}_{12}$ and its role in the decomposition of LiBH_4 . *J. Am. Chem. Soc.* **2013**, *135*, 6930–6941.

(15) Hueso, K. B.; Armand, M.; Rojo, T. High temperature sodium batteries: status, challenges and future trends. *Energy Environ. Sci.* **2013**, *6*, 734–749.

(16) Li, H.-W.; Orimo, S.-i.; Nakamori, Y.; Miwa, K.; Ohba, N.; Towata, S.; Züttel, A. Materials designing of metal borohydrides: Viewpoints from thermodynamical stabilities. *J. Alloys Compd.* **2007**, *446*, 315–318.

(17) Nickels, E. A.; Jones, M. O.; David, W. I.; Johnson, S. R.; Lowton, R. L.; Sommariva, M.; Edwards, P. P. Tuning the decomposition temperature in complex hydrides: synthesis of a mixed alkali metal borohydride. *Angew. Chem., Int. Ed.* **2008**, *47*, 2817–2819.

(18) Ley, M. B.; Ravnsbæk, D. B.; Filinchuk, Y.; Lee, Y.-S.; Janot, R. l.; Cho, Y. W.; Skibsted, J.; Jensen, T. R. $\text{LiCe}(\text{BH}_4)_3\text{Cl}$, a new lithium-ion conductor and hydrogen storage material with isolated tetranuclear anionic clusters. *Chem. Mater.* **2012**, *24*, 1654–1663.

(19) Verdál, N.; Her, J.-H.; Stavila, V.; Soloninin, A. V.; Babanova, O. A.; Skripov, A. V.; Udovic, T. J.; Rush, J. J. Complex high-temperature phase transitions in $\text{Li}_2\text{B}_{12}\text{H}_{12}$ and $\text{Na}_2\text{B}_{12}\text{H}_{12}$. *J. Solid State Chem.* **2014**, *212*, 81–91.

(20) Her, J.-H.; Yousufuddin, M.; Zhou, W.; Jalisatgi, S. S.; Kulleck, J. G.; Zan, J. A.; Hwang, S.-J.; Bowman, R. C.; Udovic, T. J. Crystal structure of $\text{Li}_2\text{B}_{12}\text{H}_{12}$: a possible intermediate species in the decomposition of LiBH_4 . *Inorg. Chem.* **2008**, *47*, 9757–9759.

(21) Paskevicius, M.; Pitt, M. P.; Brown, D. H.; Sheppard, D. A.; Chumphongphan, S.; Buckley, C. E. First-order phase transition in the $\text{Li}_2\text{B}_{12}\text{H}_{12}$ system. *Phys. Chem. Chem. Phys.* **2013**, *15*, 15825–15828.

(22) Bertheville, B.; Low, D.; Bill, H.; Kubel, F. Ionic conductivity of Na_2S single crystals between 295 and 1350 K experimental setup and first results. *J. Phys. Chem. Solids* **1997**, *58*, 1569–1577.

(23) Allis, D. G.; Hudson, B. S. Inelastic neutron scattering spectrum of $\text{Cs}_2[\text{B}_{12}\text{H}_{12}]$: reproduction of its solid-state vibrational spectrum by periodic DFT. *J. Phys. Chem. A* **2006**, *110*, 3744–3749.